A Software-Defined Radio Analysis of the Impact of Dynamic Modulation Scaling within Low-Power Wireless Systems

Arda Gumusalan, Robert Simon, Hakan Aydin
Department of Computer Science
George Mason University
Fairfax, VA - 22030
{agumusal,simon,aydin}@gmu.edu

ABSTRACT

Dynamic Modulation Scaling (DMS) is a well-known mechanism that can effectively exploit the tradeoff between communication time and energy consumption. In recent years a number of studies have suggested that DMS techniques can reduce energy consumption while maintaining performance objectives in low-power wireless transmission technologies such as those defined in IEEE 802.15.4. These studies tend to rely on theoretical or simulation DMS models to predict network performance metrics. However, there is little, if any, work that is based upon empirically verified network performance outcomes using DMS. This paper fills that gap. Our contribution is four-fold; first, using GNU Radio and SDR hardware we show how to emulate DMS in low power wireless systems. Second, we measure the impact of varying Signal-to-Noise levels on throughput and delivery rates for different DMS control strategies. Third, using DMS we quantify the impact of distance and finally, we measure the impact of different elevations between sender and receiver on network performance. Our results provide an empirical basis for future work in this area.

KEYWORDS

Low Power Lossy Networks, Dynamic Modulation Scaling

ACM Reference Format:
Arda Gumusalan, Robert Simon, Hakan Aydin. 2018. A Software-Defined Radio Analysis of the Impact of Dynamic, Modulation Scaling within Low-Power Wireless Systems. In *21st ACM International Conference on Modelling, Analysis and Simulation of Wireless and Mobile Systems (MSWIM '18), October 28-November 2, 2018, Montreal, QC, Canada.* ACM, New York, NY, USA, 10 pages. https://doi.org/10.1145/3242102.3242131

1 INTRODUCTION

DMS, also known as Adaptive Modulation, is a technique which manipulates the constellation size of a modulation schema in order to change the transmission time and energy consumption. Higher (lower) number of bits transmitted per symbol reduces (increases) the transmission time. However, encoding more bits per symbol with constant bit error rate requires an increase in the transmission output power. DMS is commonly used in many telecommunications systems and offers great potential in low-power communication in terms of reducing energy consumption and/or increasing packet delivery rate, especially for applications requiring high data rates over long ranges [24]. For instance, IEEE 802.15.4k, also known as LECIM [25], aims to establish connections up to 20 km. The choice of modulation for LECIM is the Gaussian Frequency Shift Keying (GFSK). The authors of [24] emphasize the need for carefully selecting the modulation technique; an example is deciding between GFSK, Binary Phase Shift Keying (BPSK) and Offset Quadrature Phase Shift Keying (O-QPSK). DMS is also a core component of IEEE 802.11ah which supports BPSK, QPSK, 64-QAM (Quadrature Amplitude Modulation), and 256-QAM [7]. It must be noted that higher modulation sizes used in high data rate applications bring higher Signal-to-Noise Ratio (SNR) requirements.

On the medium-to-low data rate applications, IEEE 802.15.4 is one of the standards that define physical and data link layers for low-power networks. It is widely adopted by Wireless Sensor Networks (WSNs). Despite its inherent potential for energy savings and hence increased sustainability, DMS is not part of IEEE 802.15.4 and there does not exist any off-the-shelf commercially available IEEE 802.15.4 compliant DMS-capable radio..

A detailed description of existing work on DMS is presented in Section 2. In particular, DMS has been the subject of several research articles in the Wireless Sensor Network (WSN) domain. However, due to the lack of commercially available hardware, these evaluations were typically conducted via simulation and/or using the pre-supposed closed-form energy scaling formulas. **This paper aims to fill the gap in the empirical analysis of DMS when applied in the WSN domain**. We are particularly interested in investigating the following question: Given a set of environmental conditions, modulation techniques and power levels, how do the packet delivery rates change with DMS?

We have used the Ettus B210 Software Defined Radios [20] (SDRs) and configured them according to the IEEE 802.15.4 base band, symboling rate, data rate and samples per symbol settings. Working on this configuration, we make the following contributions. First, we show how to emulate DMS in low-power networks using existing GNU Radio blocks and SDR hardware. We also provide a detailed look into the signal recovery process which may be used for future researchers to extend our work. The next three contributions model various types of environmental transmission conditions which may affect wireless systems. We vary the Signal-to-Noise-Ratios (SNRs) of channel within {2, 4, 8, 16}-PSK and DPSK modulations to assess how packet delivery rates (PDRs) change. This experiment gives a detailed insight on how the output power can be managed to

MSWIM '18, October 28-November 2, 2018, Montreal, QC, Canada

ACM ISBN 978-1-4503-5960-3/18/10...$15.00
https://doi.org/10.1145/3242102.3242131

achieve the desired PDR. These tests required a controlled noise environment with a noise generator, and therefore was conducted using Faraday Cages. We compare our findings with what existing general theoretical models suggest. We conclude that the necessary energy increase is greater than what the models suggest when we increase the modulation levels. Furthermore, we repeat the same experiments with Differential-PSK and report a very significant increase in performance. We then conduct a set of distance tests for {2, 4, 8}-DPSK and measured PDRs for distances up to 100 meters. Distance tests are of utmost importance for multi-hop networks and provide great insight on how it can be used to set up more energy- and/or latency-aware topology control. Finally, we test the impact of elevation difference between transmitter and receiver which is a common scenario for applications such as residential sensor monitoring, where some nodes are placed on tall objects.

2 RELATED WORK

The pioneering work presented in [21] led many researchers to consider DMS as an important leverage tool for low-power wireless communication. The authors presented the underlying principals of DMS and demonstrated how it can be used as an energy management technique. Some of these techniques are presented in Section 3. In the same paper, the authors also propose packet scheduling algorithms for real-time and non-real-time communication using DMS.

The work in [10] proposes modulation optimization algorithms for MQAM and MFSK schemes. The authors first break down the overall energy consumption of DMS into each hardware component's energy consumption and then analyze energy consumption per bit for different modulation levels. This paper was also one of the first to point out that the effectiveness of DMS depends on transmission distances. It has been shown that for sufficiently large distances, the lowest modulation level is the most energy efficient. However, for shorter distances this may not be the case, considering the increased weight of electronic circuitry consumption compared to that of the wireless radio.

DMS has also been studied in the Wireless Sensor Network (WSN) domain, and this is the main focus of our paper. Authors in [26] studied integration of DMS into real-time data gathering for tree-topology based WSNs. They proposed an offline optimization algorithm as well as a distributed online algorithm for efficient modulation level assignments and their simulation results have shown up to 90% energy savings. However, the proposed solutions were not applicable to TDMA-based protocols and assumed very minimal collision detection delay with light-weight traffic scenarios.

The work in [27] incorporated DMS into tree-topology based WSNs. The novelty of the paper came from combining energy harvesting with optimal modulation level selection. The authors proposed a centralized optimal as well as a distributed near-optimal solution.

The authors of [12] proposed a slack generation and reclamation mechanism for real-time WSNs. They computed slack by analyzing data redundancies and by eliminating redundant data transmissions. They then used this slack time to lower the modulation levels to reduce energy consumption while meeting deadlines. The same research group later formulated joint scheduling of computation and communication tasks with DVS and DMS respectively, as a Mixed Integer Linear Programming problem in [13]. They also proposed a polynomial-time heuristic and compared it against the optimal solution.

In [6], the authors applied DMS into cluster based WSNs with probabilistic workloads. For this scenarios, they formulated an optimal modulation level assignment to minimize overall energy consumption while meeting the deadlines. The same group later formulated optimal modulation level assignment for cluster based topologies while taking energy harvesting information into account. They have also proposed several polynomial-time algorithms and compared against the optimal solution.

The work presented in [14, 15] also studied optimal modulation level assignment for cluster based WSNs with probabilistic workload information. The authors proposed an efficient low-power-listening mechanism to dynamically reallocate available slack times which the nodes can use to lower their modulation levels.

The above papers, while important, exhibit a number of limitations. First, the modulation schema that have been used in the performance evaluations is primarily and mainly Quadrature Amplitude Modulation (QAM). However, only 16-QAM was recently added to the IEEE 802.15.4-2015 standard [23]. It is possible that the selection of QAM in the vast majority of the DMS papers followed from the use of QAM theoretical energy scaling equations in pioneering research papers [10, 21], coupled with the absence of DMS capability in off-the-shelf commercially available low-power radios. In Section 4, we show our real world test results and how they differ from what the generalized mathematical formulas suggest.

The IEEE 802.15.4 standard specifies many modulations for its physical layer, including DSSS-OQPSK, MSK, FSK, ASK, GFSK, SUN-OFDM, and MPSK [23]. More recently, at the sub-GHZ level there are a number of commercially available radios starting to be offered with support to different modulation methods. These include GFSK, FSK, OOK, and MSK modulations [17].

Other work has been performed using SDR to analyze the impact of DMS. This includes using SDRs in Inter-Vehicle Communication domain [7]. This work has analyzed BPSK, QPSK, 16-QAM, and 64-QAM in 802.11p stack. The authors reported the signal-to-noise ratios and corresponding packet-delivery-ratios for each modulation schema used. These tests were set up according to IEEE 802.11p standard where the underlying modulation is OFDM and the aforementioned modulation schemas are used as modulation mapping [2].

3 A DMS PRIMER

In this section we explain the fundamental underlying principals of DMS. In essence, DMS exploits the tradeoff between transmission time and energy consumption by controlling the number of bits encoded per symbol. Increasing (decreasing) the number of bits encoded per symbol decreases (increases) the transmission time but requires higher (lower) transmission energy consumption.

The energy consumption part is divided into two parts; energy consumption from transmission denoted as p_s, and electronic circuitry consumption denoted as p_e. They are defined in Equation (1) [21]:

Modulation scheme:	2^b-QAM	2^b-PSK	2^b-PAM
$\phi(b)$:	$2^b - 1$	$(\sin \frac{\Pi}{2^b})^{-2}$	$\frac{2^{2b}-1}{3}$

Table 1: Scaling functions

$$\begin{aligned} p_s &= C_s.\phi(b).R_s \\ p_e &= C_e.R_s \end{aligned} \tag{1}$$

Above, R_s is the number of symbols transmitted per second, b is the modulation size, C_e and C_s are constants that depend on the hardware, as well as the current environmental conditions such as atmospheric conditions, transmitter-receiver distance and temperature. $\phi(b)$ is the scaling function given in Table 1, as suggested in [21]. As can be seen, the specific increase in the energy consumption depends on the modulation technique in use.

Transmission time is independent of the modulation technique; it only depends on the symbol rate and modulation size. The time to transmit a single bit is formulated as $t_{bit} = \frac{1}{b.R_s}$ where R_s is constant and equals 62,500 symbols/second for IEEE 802.15.4 [23]. Hence, the energy consumption to send a single packet can be expressed as in Equation (2), where L_{packet} is the length of a packet in bits.

$$\begin{aligned} e_{packet} &= L_{packet}.(p_s + p_e).t_{bit} \\ &= \frac{L_{packet}.(C_s.\phi(b) + C_e)}{b_{i,k}} \end{aligned} \tag{2}$$

4 EXPERIMENTAL METHODOLOGY

We perform our Software Defined Radio (SDR) experiments on the Ettus USRP B210 radio [20]. SDRs differ from traditional radios by implementing various components such as amplifiers, modulators/demodulator, filters on a software layer rather than hardware. This offers higher configurability and flexibility.

The software we used is built using the GNU Radio, an open source platform that comes with a number of reusable *blocks*. Figure 1 shows our transmitter and receiver implementation. PSK modulation and demodulation blocks were already implemented and are explained below. Our data source is a text file consisting of randomly generated ASCII characters. The subsequent blocks shown in Figure 1 are needed to packetize the data from the source file. We have chosen 128 bytes as the packet payload length in order to comply with the IEEE 802.15.4 standard. Packetizing and tagging the input flow allow the receiver to distinguish between data from noise and other communications. We have also appended a 32-bit CRC to make sure we consider only successfully received packets after the demodulation phase.

In general, in order to successfully demodulate a signal with PSK, there has to be a signal recovery process preceding demodulation as demonstrated in Figure 2. The PSK demodulation block already has signal recovery embedded in it with adjustable parameters. However, it only outputs the demodulated data, not the recovered signal. For the demonstration purposes, we have created a signal recovery process as described in [5].

Figure 3 shows the implementation of a signal recovery process with the existing GNU Radio blocks and only one of the many possible techniques. Figure 4 shows the constellation display of QPSK-encoded signal before and after the recovery process. Here *Polyphase Clock Sync* is used for timing recovery, inter-symbol-interference, and downsampling of sampling rate from 4 samples per second to 1 sample per second. The *CMA Equalizer* block is used to react to multipath fading and as the final step the *Costas Loop* block is used to correct phase and frequency offset. Even though this signal recovery process could successfully lock the constellation points, it may have locked them with a 0, 90, 180 or 270 degrees difference, a problem going forward with demodulation. There are two ways to fix this. The first is to have a predetermined *access code* and try each of the possible phase difference to see which one decodes successfully. The second is to use *Differential PSK* (DPSK) instead. DPSK only transmits the phase shift difference as reference to the previously submitted signal. Hence, no matter what the phase difference between recovered and transmitted signal is, the relative phase difference between consecutive phase shifts still holds.

Before we present the results, we would like to elaborate more on our experience with the aforementioned PSK demodulation block's performance, as potential hints for future testbed implementations. First, in order to have successful communication, we always had to start the sender first and then the receiver; doing the the other way around with significant delays prevented the receiver from recovering the signal. We have also observed that it is not always advisable to set the transmitter and receiver channel gain values equally. In some cases, especially for higher modulation levels, we have observed a lower receiver gain (compared to the transmitter gain) yielded higher performance especially for noisy enviroments. Last but not least, it is very helpful to set the PSK Demod block parameters as real-time configurable variables which can be tested on the fly and adjusted accordingly for each modulation level and current environmental conditions.

For our testing, we have configured our Ettus B210 Radios to use 915 MHz center frequency and 62,5 ksymbol/second symbol rate. We have also used 4 samples/second which gave a total of 250 kb/second data rate (for BPSK and QPSK 2 samples/second also worked well). The 915 MHz ISM band was chosen due to its higher output power levels compared to 2.4 GHz center frequency with the same output amplifier gain.

Our primary objective was to obtain empirical indicators for energy consumption at different modulation levels. To achieve this, we have measured the necessary transmission power output with different noise levels to establish reliable communication. In order to have a noise-controlled environment and eliminate the effect of moving objects, we used Faraday Cages shown in Figure 5.

We have used a total of three Ettus B210 SDRs, one sender, one receiver, one noise generator. We have placed the sender and noise generator at equal distances from the receiver to make sure signal and noise powers are equally affected by the distance (Figure 5a).

5 EXPERIMENTAL RESULTS

In this section we present the experimental results. Using these results, we also provide some suggestions for future work in power management and reliability (in terms of packet delivery rates).

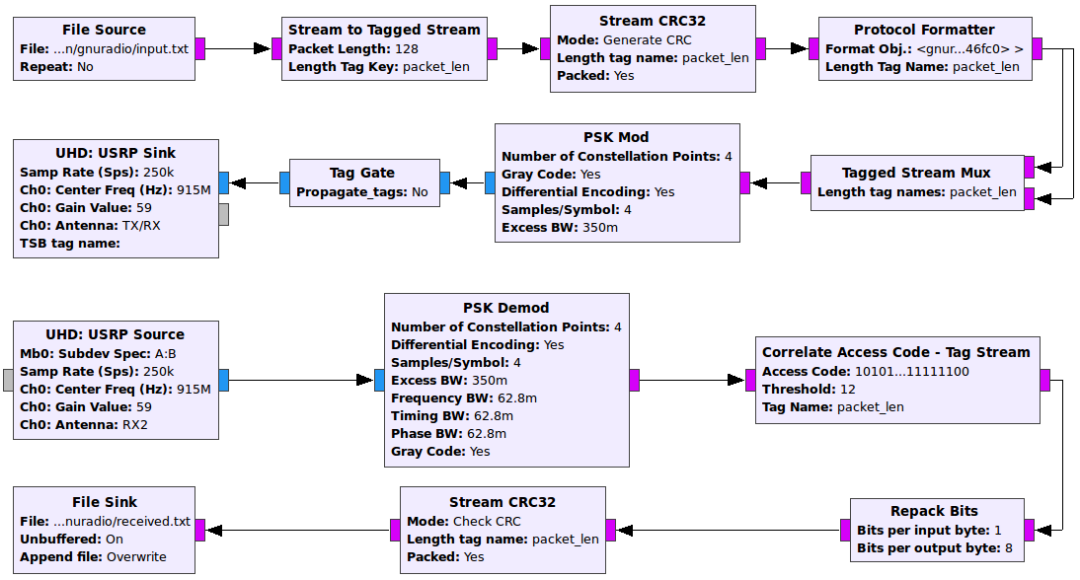

Figure 1: Implementation of transmitter and receiver in GNURADIO

Figure 2: Steps of signal decoding

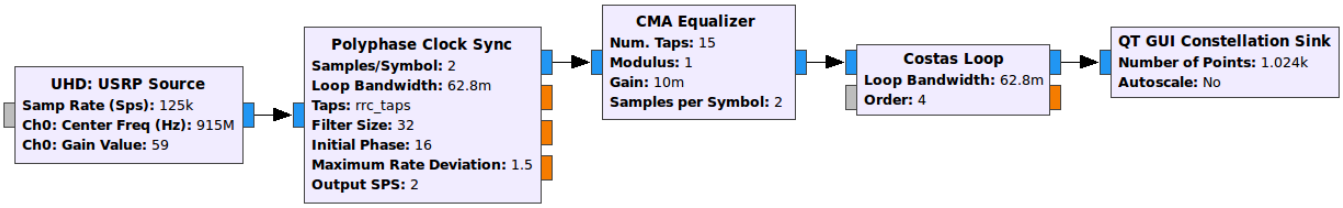

Figure 3: An example PSK signal recovery process

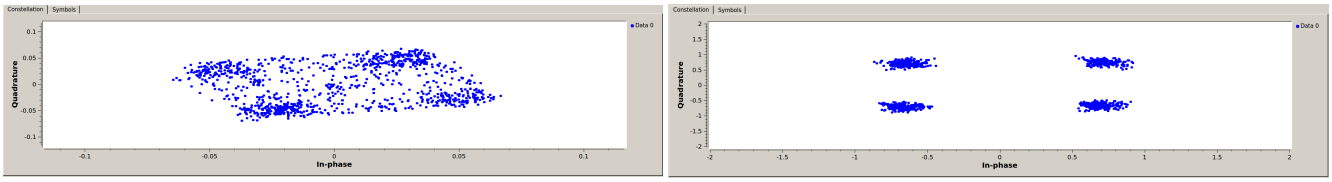

(a) Received signal **(b) Recovered signal**

Figure 4: Constellation display of received QPSK signal before and after recovery process.

5.1 Signal-to-Noise-Ratio Testing

Most of the previous work involving DMS with low-power wireless communication tends to assume constant energy output levels for each modulation level and does not take into account the fact that the output energy consumption can be controlled independently of the modulation level adjustments, in particular by varying the output amplifier gain. To better understand this issue we have measured signal-to-noise-ratios (SNRs) of MPSK modulation and the corresponding packet-delivery-rate (PDR), by varying the amplifier gain but keeping the modulation level fixed. Here, higher SNR values imply higher transmission power consumption. Our primary

(a) Inside look **(b) Outside look**

Figure 5: Faraday Cage setup

goal in this set of experiments is to anticipate the energy increase involved in guaranteeing a reliable communication with different modulation levels and various output power levels using the MPSK modulation.

Each test involved sending 300KB of payload. In order to make sure the results were minimally affected by our design, we created a *control case* by averaging how much data we can decode without any noise using the second modulation level. Hence, we have compared the amount of the data received to this control case value to compute the reported PDR values. The control case was never able to receive all of the 300KB of data. The highest we could decode was 99.9%. This is because the signal recovery process takes a while and loses some of the initial data. This can be fixed by sending a data link layer preamble before the data packets or creating a more robust and optimized demodulation process. We believe the latter will be the case when DMS-compliant low-power radios are commercially available. Each PDR point is averaged over 100 experiments. Lastly, we have adjusted the noise level to at 10% of the maximum analog gain of Ettus B210 radios (max gain is 89.8 dB) and adjusted transmission gains accordingly to create the desired SNR ratio. For the SNR ratios greater than 10 times, we have reduced the noise level. The receiver gain values varied across the different settings. Hence, the reported increases in transmission power are only for the transmitter but a close approximation for the receiver.

Figure 6 shows the results obtained for {2, 4, 8, 16}-PSK. In addition, we have also plotted the theoretical values obtained for {4, 8, 16}-PSK using the scaling function reported in Table 1 by using 2-PSK as the base case. We can see a marked difference between the theoretical predictions and empirical measurements. In order to have at least an average PDR of 99% 2-PSK required an SNR of 4. For 4-PSK, this value increased by a factor of 6 (to 12). However, the scaling function suggests only an increase of 4 times. 8-PSK required an SNR of 16, an increase of 2.5 times over 8-PSK, which is much lower than what the scaling function suggests. Unfortunately for 16-PSK case, the best we could received was an average of 33% PDR (we were unable to achieve a PDR of 35% even in the absence

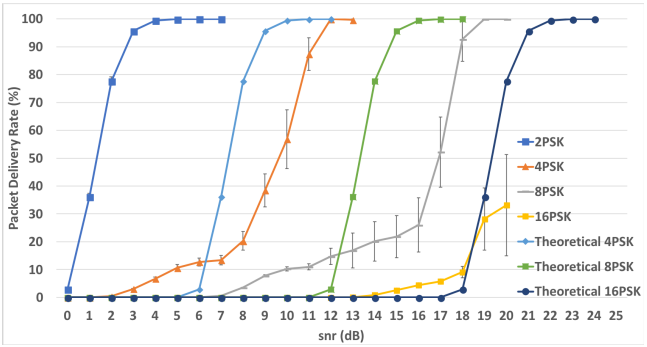

Figure 6: SNR to PDR comparison of empirical measurements and theoretical calculations for MPSK

of noise). This may be due to not having enough output power level and as well as low performance of signal recovery process of built in PSK demodulation for higher constellation sizes also the noise generated by the transmitting SDR and the internal noise of the receiving SDR's hardware. However, if we compare this 33% PDR value to 8-PSK, a 2.5 times increase is observed, once again a value lower than what the scaling function suggests.

Next, we repeated the same experiments with Differential-PSK (DPSK) modulation. It has been shown that in communications over fading channels DPSK is preferable over PSK. DPSK uses the previously transmitted symbol interval's phase as a reference to decode the current symbol interval. In channels with slow condition variations compared to the symboling rate, DPSK gives good performance [16] [11].

Figure 7 validates the better performance of DPSK over PSK. The results of 2-DPSK and 2-PSK were very close and both required an SNR value of 4 to have at least a 99% delivery rate. The major difference is observed for {4, 8, 16} DSPK. 4-DPSK achieved 99% PDR for SNR = 5 and required roughly 1.25 times more output gain compared to 2-DPSK. This value was 6 for 4-PSK. 8-DPSK

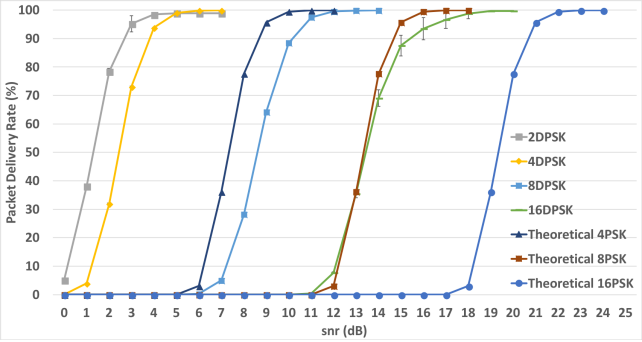

Figure 7: SNR to PDR comparison of empirical measurements and theoretical calculations for MDPSK

achieved the same PDR for of 12 which is 5 times the output gain compared to 4-DPSK. However, it only required 6 times the output gain of 2-DPSK. Lastly, 16-DPSK also required 5 times more output gain compared to 8-DPSK. {4, 8, 16} DSPK all performed better than the theoretical PSK results as expected; 31%, 39%, 50% of the theoretical results, respectively. A final conclusion can be drawn from both Figure 6 and 7; we can see that the scaling ratios between consecutive modulation levels vary and are not a constant value.

Translation from the results reported in Figure 6 and Figure 7 to the exact energy consumption of an IEEE 802.15.4compliant radio will depend on the hardware design (the constants mentioned in Section 3), efficiency of the demodulation technique, as well as the channel access algorithm. As with many wireless standards, the 802.15.4 data link layer has two operating modes: The *beacon* mode and *non-beacon* mode. *Beacon* mode consists of two phases; *contention allowance period* (CAP) and *contention free period* (CFP). During CAP the nodes use slotted-CSMA to get an access to channel and in CFP the nodes have guaranteed time slots where the nodes take turn for channel access in time division multiple access fashion. *Non-beacon* mode is a simple CSMA access mechanism. For both cases the nodes assess the current noise level in the channel before transmitting. Since our reported results are based on SNR values, lower noise levels will require lower output power. However, the increase in power consumption between different modulation levels will remain valid for a given noise level.

We now consider a real-world case where using SNR indications to predict energy consumption may be quite useful. Protocols for Wireless Industrial Control Networks (ICNs) such as WirelessHART or ISA 100.11a require real-time packet delivery with application specific packet delivery rate requirements. Wireless ICN protocols typically uses time-division-multiple-access based channel access mechanism with primary and backup time slots for reliability [3, 18, 22]. In an application where a 98% PDR is the goal, SNR-based output power control provides a very fine tuned energy control mechanism. In this scenario rather than aiming for 98% or above delivery rate with a single transmission, aiming for a lower PDR and retransmitting in case of a packet loss may give a lower expected energy consumption. For example, if we are aiming for at least a 98% PDR using 16-DPSK, we can either use an SNR value of 18 and transmit only once or use 15 (88% PDR) with a retransmission if it fails. In the latter, we will have to retransmit with a probability of 12% which will give a total of 98.56% PDR. Using an SNR of 18 with a single transmission will consume 1.78 times more energy as opposed to the expected energy consumption of using 15 with retransmission. Integrating DMS into this scenario gives the application the ability to not only fine tune its output power level but also take advantage of available transmission delay. An application can use a lower modulation level as long as the time slot length is large enough. Let us assume the primary time slot requires modulation level 16 whereas the backup slot can compensate for 8 (twice as long). Once again aiming for 88% PDR in both time slots for an expected PDR of 98% will consume 52% of a single transmission energy consumption.

We also suggest a slightly different perspective to the application of DMS in the low-power wireless domain. The primary focus of DMS-enabled low-power protocols has been energy management, and DMS is utilized as a tradeoff between time and energy while keeping PDR constant. In other words the goal is to manage output power while achieving the same PDR. However, it is also possible to view DMS as a mechanism that provides a tradeoff between time and reliability (in terms of packet delivery rates). In other words, DMS can be used to keep the output power constant while reducing the modulation level in order to achieve the same or higher PDR. For example, let us assume we have a sensor mote which is currently using 8-DPSK and achieving 97% PDR with a SNR value of 11. Now assume that there is a sudden change in channel condition which reduced our SNR value to 7. Instead of increasing the output power to restore SNR value back to 11, the mote can decrease its modulation level to 4 and still achieve 97% and above PDR while using the same output power level as long as the latency requirements are not violated. Even in non-changing channel conditions where SNR ratio is fairly constant, if the current quality-of-service requirements of the application-layer protocol changes and requires a higher PDR, it is still achievable with the same transmission power by decreasing the modulation level rather than increasing output gain. We believe this type of DMS application is just as important and offers a viable direction for the future research of DMS in low-power wireless networks.

5.2 Distance Testing

In the next set of experiments, we evaluated the impact of distance on PDR, for M-DPSK. Distance testing is important due to its impact on topology control. In wireless domains, topology control is mainly used to find an optimal subset of the nodes in the network to ensure connectivity. Notice that connectivity may have slightly different meaning in the low-power domain, so here we are referring to the ability that each sensing node can successfully communicate with the coordinator with or without using relay nodes. One important advantage of this approach is that nodes can better manage their sleep schedules [4]. DMS gives the ability to control the transmission distance without increasing the output power consumption but with a penalty of increased transmission delay.

Figure 8 shows the picture of the test area. We chose this location because it was very isolated and we measured very weak WiFi

Figure 8: The test area that was used for distance measurements. Sender and receiver are 100 meters apart.

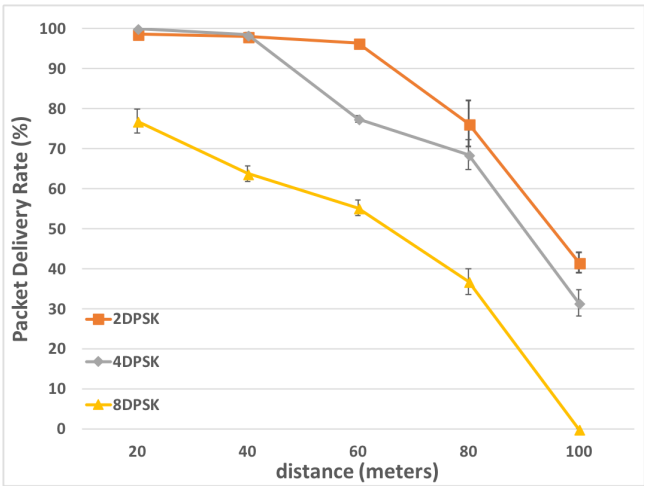

Figure 9: Packet delivery rates for different modulation levels using 2.4 GHz center frequency with 70dB output amplifier gain in terms of distance.

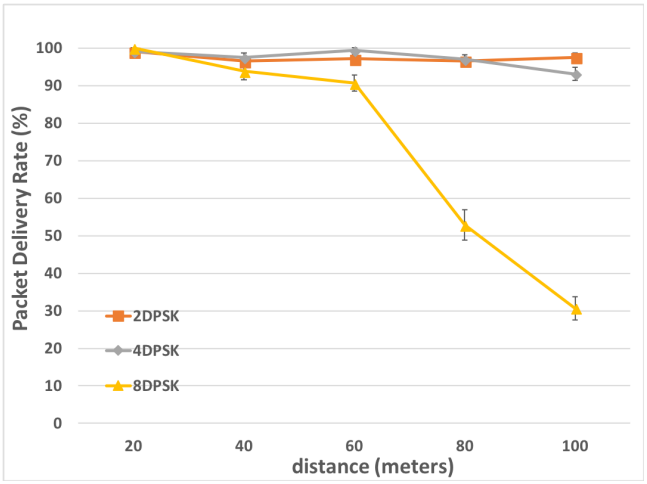

Figure 10: Packet delivery rates for different modulation levels using 915 MHz center frequency with 70 dB output amplifier gain in terms of distance.

activity. Also, it allowed us to test up to 100 meters. The location of the receiver was chosen in such a way that the multi-path fading was minimal and it was located in the exact same spot for each test. The location of the sender was adjusted accordingly for each desired distance on a straight line.

Our first experiment was conducted in the 2.484-GHz center frequency with the same parameters used for the SNR tests. Low-power radios such as CC2420 has 0 dBm maximum transmission power. Hence, our goal was to set our SDRs to use 0 dBm output power as well. However, SDR only allows us to configure its output amplifier gain (in dB) which produces different absolute transmission power levels depending on the center frequency in use. In order to get very accurate mapping of output amplifier gain to the absolute transmission output power, spectrum analyzer and highly sensitive power monitors are needed. We identified a forum post on the official National Instruments website by a SDR Product manager of the company, which provided their internal test results of mapping amplifier gain to specific output power for different center frequencies using the Ettus B200 series SDRs [1]. According to their internal test results an amplifier gain between 61 dB and 75 dB corresponds to 0 dBm output power. In order to pinpoint a specific gain value within this range, we have measured RSSI values with Zolertia Z1 motes set as sender and receiver equipped with CC2420 radios transmitting at 0dBm. Next, we have repeated the same test with the same Z1 receiver instead of Ettus B210 transmitter. An output gain of 70dB gave the closest RSSI values to match 0 dBm absolute transmission output power.

Figure 9 shows the results we obtained for {2, 4, 8}-DPSK. We were unable to decode any signal using 16-DPSK with 70 dB output amplifier gain. The error bars seen on the graph indicate 95% confidence levels. From these tests, we can conclude that increasing modulation levels decreases PDR at a specific distance.

We then repeated the same test with the 915-MHz center frequency. National Instruments internal tests indicate 70 dB amplifier gain corresponds to a little less than 10 dBm output power. Similarly, Texas Instruments sub-1-Gig low power radios have around 10 dBm maximum output power as opposed to 0 dBm of CC2420 2.4 GHz radio. As expected PDR, has increased with increasing distance for each modulation level significantly. In fact, both 2- and 4-DPSK has maintained above 90% delivery rate for up to 100 meters. This increase is due to the aforementioned increase in the output power level. For a good measure of comparison we ran tests with 915 MHz but this time with 60 dB amplifier gain. This gain value corresponded approximately to 0 dBm according to National Instruments internal tests [1]. However, this time we did not have a sub-1gig radio to compare RSSI values. We have observed similar but slightly better results compared to 2.4 GHz. This was likely due to a combination of slightly higher output power level created by 60 dB gain 915 MHz center frequency as opposed to 70 dB 2.4 GHz

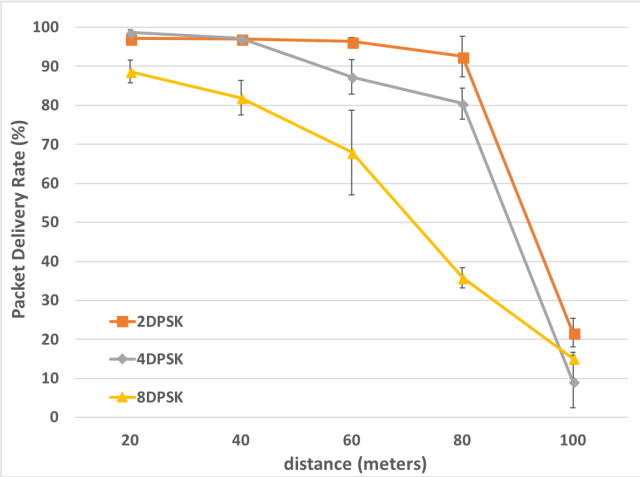

Figure 11: Packet delivery rates for different modulation levels using 915 MHz center frequency with 60 dB output amplifier gain in terms of distance.

Figure 12: Test area used in for elevation tests. The receiver is placed on the ground and the sender is elevated.

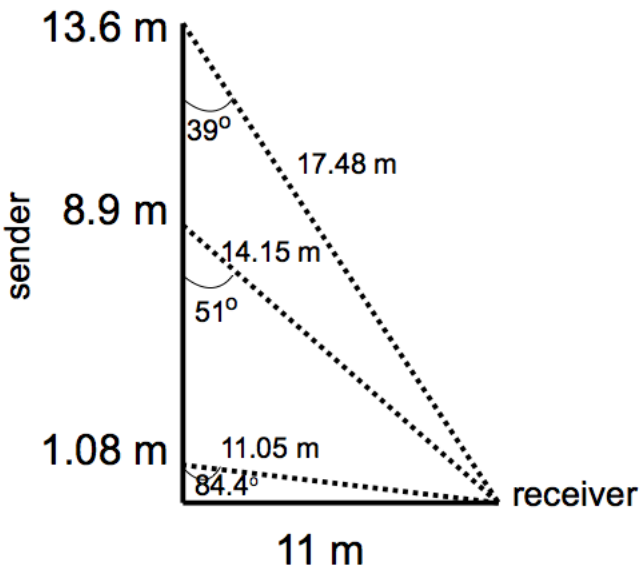

Figure 13: The height of the sender and the distance of the sender from the receiver.

and lower free space propagation loss of 915 MHz band as opposed to the 2.4 GHz band [19].

These results have important implications for topology control. Connection driven topology control protocols such as Span [9] and ASCENT [8] aim to find the minimum number of relay nodes necessary to forward packets to the coordinator. The goal is to reduce the number of active nodes and hence the number of hops. Lowering modulation level allows approaches that work by enabling nodes to broaden their communication range while reducing their energy consumption. As a result, these similar topology control protocols can further reduce the number of active relay nodes. Assume an example where a sensing node is 120 meters away from the coordinator and needs 2 relay nodes positioned 40 meters apart to forward its packets using modulation level 4. According to our tests, reducing modulation level to 2 will increase the reliable communication range up to 60 meters and only a single relay node will be sufficient to forward the packets. Here, the total energy savings will be the sum of *energy saving from the sensing node, relay node and coordinator by reducing their modulation levels* and *energy savings by putting a relay node into deep sleep*, a figure which may be quite significant.

5.3 Elevation Testing

In our last set of experiments, we have measured the PDR values of {2, 4, 8}-DPSK with varying elevation difference between sender and receiver. We have placed the sender outside of a building at 1.08m, 8.9m, and 13.6m high in reference to the receiver. The receiver is placed on the ground level (slightly elevated). Figure 12 shows the tests area and Figure 13 shows the height of the sender and the distance between sender and the receiver. In applications such as residential automatic meter reading, it is possible for sender and receiver to have elevation difference – for example, a transmitter can be placed on a current-meter which may be above the ground or an elevated pipeline equipped with sensors may broadcast the current pressure inside the pipes.

Figure 14 shows the PDR of {2, 4, 8}-DPSK with 915-MHz center frequency and 60 dB output amplifier gain as we have used in Section 5.2. Some conclusions we draw can be listed as follows: (i) Higher elevations cause higher packet loss for both 915 MHz and 2.484 GHz center frequency although 2.484 GHz center frequency with 70 dB output amplifier gain had higher PDR for both 4 and 8 -DPSK as shown in Figure 15. We should mention here that we were using different antennas for 915 MHz and 2.484 GHz tests that are

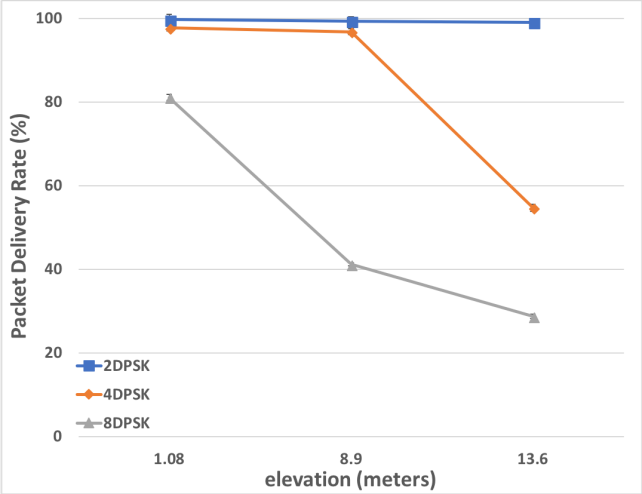

Figure 14: Packet delivery rates for different modulation levels using 915 MHz center frequency with 60 dB output amplifier gain in terms of elevation difference.

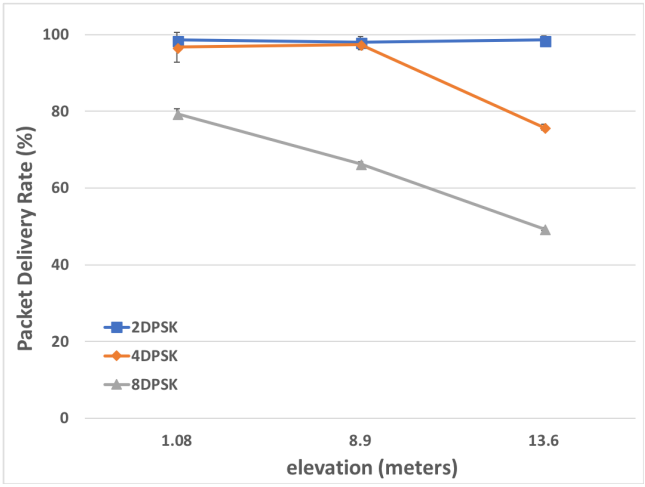

Figure 15: Packet delivery rates for different modulation levels using 2.484 GHz center frequency with 70 dB output amplifier gain in terms of elevation difference.

both omni-directional vertical antennas (Ettus Research VERT900 and VERT2450 respectively). Different antennas may have different polarization characteristics typically either vertical, horizontal or circular in x-y axis. Elevation difference requires the signals to be transmitted in the z axis where VERT900 and VERT2420 antennas likely to have different characteristics in this direction. (ii) 2-DPSK seems to be not effected by the elevation difference with the tested output gain values making it the best candidate for the aforementioned types of applications. (iii) If we compare the results from Figures 14 and 15 with Figures 9 and 11, we observe that elevation difference has a higher impact on PDR compared to distance difference at the same elevation. Figures 9 and 11 indicates that all the modulation levels have 80% or above PDR for distances up to 20 m (with no elevation difference) whereas when the transmitter is elevated 13.6m and placed 17.48 m apart from the receiver, the PDR reduces significantly for 4 and 8-DPSK (as low as 54% and 28%), respectively.

6 CONCLUSION

Applicability of Dynamic Modulation Scaling (DMS) in low-power wireless systems, including IEEE 802.15.4 networks, as an energy management technique has been widely studied in literature and shown that DMS can achieve significant energy savings. However, much the work that has been done so far lacks substantial empirical analysis of DMS on Wireless Sensor Networks (WSNs). As a result, only a generalized mathematical evaluation of DMS were available to the researchers. This paper addressed that gap and provides empirical results that can be used by future researchers as a complement to currently available mathematical techniques.

We used Ettus B210 Software Defined Radios (SDRs) and configured them according to the 2015 IEEE 802.15.4 standard. We experiments with various Signal-to-Noise-Ratios and corresponding Packet-Delivery-Rates for {2, 4, 8, 16}-PSK as well as DPSK modulations. Our results show that increasing PSK modulation levels requires more transmission power increase compared to theoretical scaling functions (such as those shown in Table 1). On the other hand, DPSK requires significantly *less* power increase compared to the same scaling function. We have also shown that the scaling ratios between consecutive modulation levels are not equal. Next, we measured the PDRs for {2, 4, 8}-DPSK for distances up to 100 meters. The results have shown that lower modulation levels can achieve higher communication distances. We have also shown the performance difference between 915 MHz and 2.484 GHz and observed 915 MHz has higher packet delivery rate with the same output amplifier gain. Lastly, we have shown that elevation difference between transmitter and receiver affects these results tremendously. 4-DPSK and 8-DPSK had as low as 54% and 28% PDR for elevation difference of 11.6m and 17.48m apart. The same modulations had 99% and 76% PDR respectively for distances up to 20 m with no elevation difference.

ACKNOWLEDGMENT

The authors would like to thank Dr. Duminda Wijesekera from Computer Science Department (George Mason University) for giving us access to Radar and Radio Engineering Lab's Faraday cages.

REFERENCES

[1] [n. d.]. https://forums.ni.com/t5/USRP-Software-Radio/How-to-set-the-trasmit-power-of-USRP/td-p/2202190. https://forums.ni.com/t5/USRP-Software-Radio/How-to-set-the-trasmit-power-of-USRP/td-p/2202190
[2] IEEE 802.11p 2010 Standard. [n. d.]. IEEE 802.11p-2010. https://www.ietf.org/mail-archive/web/its/current/pdfqf992dHy9x.pdf Last accessed on 2018-Feb-21.
[3] IEEE 802.15.4e Standard. [n. d.]. https://standards.ieee.org/findstds/standard/802.15.4e-2012.html Last accessed on 2017-May-22.
[4] Giuseppe Anastasi, Marco Conti, Mario Di Francesco, and Andrea Passarella. 2009. Energy conservation in wireless sensor networks: A survey. *Ad hoc networks* 7, 3 (2009), 537–568.
[5] KR Damindra S Bandara, Anthony Melaragno, Duminda Wijesekera, and Paulo Costa. 2017. A case study of cognitive radio networks: Secure spectrum management for positive train control operations. In *Spectrum Access and Management for Cognitive Radio Networks*. Springer, 121–152.
[6] Maryam Bandari, Robert Simon, and Hakan Aydin. 2016. On minimizing expected energy usage of embedded wireless systems with probabilistic workloads.

Sustainable Computing: Informatics and Systems 11 (2016), 50–62.

[7] Bastian Bloessl, Michele Segata, Christoph Sommer, and Falko Dressler. 2013. Towards an Open Source IEEE 802.11 p stack: A full SDR-based transceiver in GNU Radio. In *Vehicular Networking Conference (VNC), 2013 IEEE*. IEEE, 143–149.

[8] Alberto Cerpa and Deborah Estrin. 2002. Ascent: Adaptive self-configuring sensor network topologies. *ACM SIGCOMM Computer Communication Review* 32, 1 (2002), 62–62.

[9] Benjie Chen, Kyle Jamieson, Hari Balakrishnan, and Robert Morris. 2002. Span: An energy-efficient coordination algorithm for topology maintenance in ad hoc wireless networks. *Wireless networks* 8, 5 (2002), 481–494.

[10] Shuguang Cui, Andrea J Goldsmith, and Ahmad Bahai. 2005. Energy-constrained modulation optimization. *IEEE transactions on wireless communications* 4, 5 (2005), 2349–2360.

[11] Franz Edbauer. 1992. Bit error rate of binary and quaternary DPSK signals with multiple differential feedback detection. *IEEE Transactions on Communications* 40, 3 (1992), 457–460.

[12] Benazir Fateh and Manimaran Govindarasu. 2013. Energy minimization by exploiting data redundancy in real-time wireless sensor networks. *Ad Hoc Networks* 11, 6 (2013), 1715–1731.

[13] B. Fateh and M. Govindarasu. 2015. Joint Scheduling of Tasks and Messages for Energy Minimization in Interference-aware Real-time Sensor Networks. *Mobile Computing, IEEE Transactions on* 14, 1 (2015), 86–98.

[14] Arda Gumusalan, Robert Simon, and Hakan Aydin. 2016. Adaptive Transmission Scheduling for Energy-Aware Real-Time Wireless Communication. In *Proceedings of the 2016 International Conference on Embedded Wireless Systems and Networks (EWSN '16)*. Junction Publishing, USA, 1–12. http://dl.acm.org/citation.cfm?id=2893711.2893713

[15] Arda Gumusalan, Robert Simon, and Hakan Aydin. 2018. Flexible Real-time Transmission Scheduling for Wireless Networks with Non-deterministic Workloads. *Ad Hoc Networks* (2018).

[16] Paul Ho and Dominic Fung. 1991. Error performance of multiple symbol differential detection of PSK signals transmitted over correlated Rayleigh fading channels. In *Communications, 1991. ICC'91, Conference Record. IEEE International Conference on*. IEEE, 568–574.

[17] Texas Instruments. [n. d.]. Sub1GHz radios. http://www.ti.com/wireless-connectivity/simplelink-solutions/sub-1-ghz/products.html Last accessed on 2018-March-5.

[18] Tomas Lennvall, Stefan Svensson, and Fredrik Hekland. 2008. A comparison of WirelessHART and ZigBee for industrial applications. In *Proceedings of IEEE International Workshop on Factory Communication Systems*.

[19] Minyoung Park. 2015. IEEE 802.11 ah: sub-1-GHz license-exempt operation for the internet of things. *IEEE Communications Magazine* 53, 9 (2015), 145–151.

[20] Ettus Research. [n. d.]. Ettus USRP B210. https://www.ettus.com/product/details/UB210-KIT Last accessed on 2018-Feb-22.

[21] Curt Schurgers, Vijay Raghunathan, and Mani B Srivastava. 2003. Power management for energy-aware communication systems. *ACM Transactions on Embedded Computing Systems* 2, 3 (2003), 431–447.

[22] Jianping Song, Song Han, Aloysius K Mok, Deji Chen, Margaret Lucas, and Mark Nixon. 2008. WirelessHART: Applying wireless technology in real-time industrial process control. In *Proceedings of IEEE Real-Time and Embedded Technology and Applications Symposium*.

[23] IEEE 802.15.4-2015 Standard. [n. d.]. https://standards.ieee.org/findstds/standard/802.15.4-2015.html Last accessed on 2018-Feb-21.

[24] Hai Wang and Abraham O Fapojuwo. 2017. A survey of enabling technologies of low power and long range machine-to-machine communications. *IEEE Communications Surveys & Tutorials* 19, 4 (2017), 2621–2639.

[25] Xiong Xiong, Kan Zheng, Rongtao Xu, Wei Xiang, and Periklis Chatzimisios. 2015. Low power wide area machine-to-machine networks: key techniques and prototype. *IEEE Communications Magazine* 53, 9 (2015), 64–71.

[26] Yang Yu, Viktor K Prasanna, and Bhaskar Krishnamachari. 2006. Energy minimization for real-time data gathering in wireless sensor networks. *IEEE Transactions on Wireless Communications* 5, 11 (2006).

[27] Bo Zhang, Robert Simon, and Hakan Aydin. 2013. Harvesting-aware energy management for time-critical wireless sensor networks with joint voltage and modulation scaling. *Industrial Informatics, IEEE Transactions on* 9, 1 (2013), 514–526.